

# GPS Multipath Detection Based on Sequence of Successive-Time Double-Differences

Hyung Keun Lee, Jang-Gyu Lee, and Gyu-In Jee

Hyung Keun Lee is with Seoul National University-Korea University Joint Research Division for Information Technology, Brain Korea 21, Seoul, Korea (e-mail:hyknlee@asrignc1.ac.kr)

Jang-Gyu Lee is with the School of Electrical Engineering and Computer Science and Automatic Control Research Center, Seoul National University, Seoul, Korea (e-mail:jglee@snu.ac.kr)

Gyu-In Jee is with the Department of Electronics Engineering, Konkuk University, Seoul, Korea (e-mail:gjee@konkuk.ac.kr)

## Abstract

Based on a sequence of successive-time double-differences of pseudorange and carrier phase measurements provided by Global Positioning System (GPS), a channelwise test statistic is proposed. The proposed test statistic is particularly efficient in multipath detection and operationally advantageous in that it requires basic observables only, it does not require any pre-computation of receiver position, it has standard  $\chi^2$  -distributions, and it can reduce the detection resolution by increasing the number of successive measurements. To analyze the proposed test statistic, both minimum detectable jump and minimum detectable ramp are derived. An experiment under an intentional multipath environment exhibits the effectiveness of the proposed test statistic.

## I. INTRODUCTION

Multipath is one of the most dominant error sources of Global Positioning System (GPS). To mitigate the multipath error, test statistics to detect abnormal signal condition are often used. They are the parity vector magnitude based on pseudoranges [1,2], the signal-to-noise ratio [3,4], the instantaneous difference between the pseudorange and the carrier-phase [4,5], and the judicious linear combinations of the pseudorange and the L1 and L2 carrier-phases [6]. The identified false measurements are eliminated or de-weighted in computing the receiver's position. In using the conventional multipath test statistics for real-time kinematic GPS, difficulties arise due to insufficient detection performance [1,2,4,5] and requirement of specialized hardware [3,4,6].

To improve multipath detection performance in real-time kinematic positioning, this paper proposes an efficient Channelwise Test Statistic (CTS). The proposed CTS is based on a sequence of Successive-Time Double-Differences (STDD) of pseudoranges and carrier-phases that can be provided by a single-frequency GPS receiver. Compared with the conventional multipath test statistics, the CTS is operationally advantageous in that it requires no specialized hardware, it has a standard  $\chi^2$  -distribution whose degree of freedom can be arbitrarily chosen, and it requires no pre-computation of receiver position. It imposes no large computational burden since a pre-computed gain matrix is utilized. In addition, its availability is good since the number of visible satellites does not impose a constraint. With a slight modification, the proposed multipath test statistic can also be applied to differential positioning applications.

## II. CHANNELWISE MULTIPATH TEST STATISTIC

Consider a single-frequency GPS receiver providing pseudorange and accumulated carrier-phase measurements. The pseudorange  $\tilde{\rho}_k^j$  between the receiver and the  $j$ -th satellite at the  $k$ -th epoch can be modeled by

$$\tilde{\rho}_k^j = r_k^j + B_k + E_k^j + I_k^j + T_k^j + M_k^j + W_k^j, \quad W_k^j \sim (0, r_\rho) \quad (1)$$

where  $r_k^j$  indicates the true distance,  $B_k$  indicates the receiver clock bias,  $E_k^j$  indicates the satellite's clock error and orbit information error,  $I_k^j$  indicates the ionospheric error,  $T_k^j$  indicates the tropospheric error,  $M_k^j$  indicates the code multipath, and  $W_k^j$  indicates the code thermal noise with white Gaussian distribution.

Likewise, the instantaneous accumulated carrier-phase  $\tilde{\Phi}_k^j$  with an unresolved integer ambiguity  $\mathbf{N}_k^j$  can be modeled by

$$\tilde{\Phi}_k^j = r_k^j + B_k + E_k^j - I_k^j + T_k^j + m_k^j + w_k^j + \lambda \mathbf{N}_k^j, \quad w_k^j \sim (0, r_\Phi) \quad (2)$$

where  $m_k^j$  indicates the carrier phase multipath,  $w_k^j$  indicates the carrier thermal noise with white Gaussian distribution,  $\lambda$  indicates the carrier wave length, and  $\mathbf{N}_k^j$  indicates the unknown integer ambiguity. The code and carrier mutipath terms  $M_k^j$  and  $m_k^j$  are assumed to be independent of the thermal noise terms  $W_k^j$  and  $w_k^j$ , respectively, and generate larger fluctuations in the measurement sequences than the thermal noise terms.

To detect abnormal signal condition, an STDD  $d_i^j$  is computed. Based on Eqs. (1) and (2), the STDD  $d_i^j$  satisfies the following equation.

$$d_i^j = (\tilde{\rho}_i^j - \tilde{\rho}_{i-1}^j) - (\tilde{\Phi}_i^j - \tilde{\Phi}_{i-1}^j) = \mu_i^j + \nu_i^j \quad (3)$$

where

$$\mu_i^j := (M_i^j - M_{i-1}^j) - (m_i^j - m_{i-1}^j) + 2(I_i^j - I_{i-1}^j) - \lambda(\mathbf{N}_i^j - \mathbf{N}_{i-1}^j) \quad (4)$$

$$\nu_i^j := W_i^j - W_{i-1}^j - (w_i^j - w_{i-1}^j) \quad (5)$$

$$\begin{bmatrix} \nu_i^j \\ \nu_l^j \end{bmatrix} \sim \left( \begin{bmatrix} 0 \\ 0 \end{bmatrix}, \begin{bmatrix} \Lambda_\rho & -\frac{1}{2}\Lambda_\rho \\ -\frac{1}{2}\Lambda_\rho & \Lambda_\rho \end{bmatrix} \right) \text{ if } l = i \pm 1$$

$$\sim \left( \begin{bmatrix} 0 \\ 0 \end{bmatrix}, \begin{bmatrix} \Lambda_\rho & 0 \\ 0 & \Lambda_\rho \end{bmatrix} \right) \quad \text{if } l \neq i \pm 1 \quad (6)$$

$$\Lambda_\rho := 2(r_\rho + r_\Phi). \quad (7)$$

Except for the rare cases of ionospheric scintillation, the term  $2(I_i^j - I_{i-1}^j)$  is negligible since the correlation time of ionospheric error is on the order of hours [7]. Likewise, the term  $(\mathbf{N}_i^j - \mathbf{N}_{i-1}^j)$  is also negligible except for the occasional cases of cycle slip. Thus, in the normal signal conditions when there are no multipath, ionospheric scintillation, and cycle-slip,  $\nu_i^j$  in Eq. (5) dominates the STDD  $d_i^j$ . However, as shown in Eqs. (3)-(7), even in the normal signal conditions, the subsequent  $d_i^j$  and  $d_{i+1}^j$  are correlated. To decorrelate the STDD sequence, a stochastic orthogonalization is applied to  $\{d_i^j\}$  from the  $(k - B + 1)$ -th epoch to the  $k$ -th epoch.

$$\begin{aligned} \bar{\Lambda}_i^j &= \Lambda_i^j - \frac{1}{4} \frac{\Lambda_\rho^2}{\bar{\Lambda}_{i-1}^j}, & \bar{\Lambda}_{k-B+1}^j &= \Lambda_\rho \\ \bar{d}_i^j &= d_i^j + \frac{1}{2} \frac{\Lambda_\rho}{\bar{\Lambda}_{i-1}^j} \bar{d}_{i-1}^j, & \bar{d}_{k-B+1}^j &= d_{k-B+1}^j \end{aligned} \quad (8)$$

As a result, the orthogonalized sequence  $\{\bar{d}_i^j\}$  becomes independent Gaussian in the normal signal conditions.

$$\begin{bmatrix} \bar{d}_k^j \\ \bar{d}_{k-1}^j \\ \vdots \\ \bar{d}_{k-B+1}^j \end{bmatrix} \sim \left( \begin{bmatrix} 0 \\ 0 \\ \vdots \\ 0 \end{bmatrix}, \begin{bmatrix} \bar{\Lambda}_k^j & 0 & \cdots & 0 \\ 0 & \bar{\Lambda}_{k-1}^j & \cdots & 0 \\ \vdots & \vdots & \ddots & \vdots \\ 0 & 0 & \cdots & \bar{\Lambda}_{k-B+1}^j \end{bmatrix} \right) \quad (9)$$

Utilizing the de-correlatedness of  $\{\bar{d}_i^j\}$ , a test statistic to detect abnormal signal conditions can be recursively computed by

$$T_{k-B+1/k}^j := \sum_{k-B+1}^k \frac{(\bar{d}_i^j)^2}{\bar{\Lambda}_i^j} = T_{k-B+1/k-1}^j + \frac{(\bar{d}_k^j)^2}{\bar{\Lambda}_k^j}. \quad (10)$$

As a result, the CTS  $T_{k-B+1/k}^j$  in Eq. (10) satisfies the following statistical distributions under two hypotheses.

$$\begin{aligned} H_0 \text{ (normal)} : & \quad T_{k-B+1/k}^j \sim \chi^2(B, 0) \\ H_1 \text{ (abnormal)} : & \quad T_{k-B+1/k}^j \sim \chi^2(B, \lambda_{k-B+1/k}^j) \end{aligned} \quad (11)$$

where  $\chi^2(B, 0)$  and  $\chi^2(B, \lambda_{k-B+1/k}^j)$  denote the centralized and non-centralized chi-square distributions, respectively. As shown in Eq. (11), the total number of subsequent epochs  $B$  determines the degree of freedom (DOF) of  $\chi^2$ -distributions. The non-centrality parameter  $\lambda_{k-B+1/k}^j$  is related to the modified fault sequence  $\{\bar{\mu}_i^j\}$  as follows.

$$\lambda_{k-B+1/k}^j = \sum_{k-B+1}^k \frac{(\bar{\mu}_i^j)^2}{\bar{\Lambda}_i^j} \quad (12)$$

where the modified fault sequence  $\{\bar{\mu}_i^j\}$  from the  $(k - B + 1)$ -th epoch to the  $k$ -th epoch is related to the original fault sequence  $\{\mu_i^j\}$  by

$$\bar{\mu}_i^j = \mu_i^j + \frac{1}{2} \frac{\Lambda_\rho}{\bar{\Lambda}_{i-1}^j} \bar{\mu}_{i-1}^j, \quad \bar{\mu}_{k-B+1}^j = \mu_{k-B+1}^j. \quad (13)$$

For blockwise computation of CTS,  $D_{k-B+1/k}^j$  and  $\bar{D}_{k-B+1/k}^j$  are defined as the stacked vectors of  $d_i^j$  and  $\bar{d}_i^j$ , respectively.

$$\begin{aligned} D_{k-B+1/k}^j &:= \left[ d_k^j \ d_{k-1}^j \ \cdots \ d_{k-B+1}^j \right]^T \\ \bar{D}_{k-B+1/k}^j &:= \left[ \bar{d}_k^j \ \bar{d}_{k-1}^j \ \cdots \ \bar{d}_{k-B+1}^j \right]^T \end{aligned} \quad (14)$$

According to Eqs. (8) and (14),  $D_{k-B+1/k}^j$  and  $\bar{D}_{k-B+1/k}^j$  satisfy

$$\begin{aligned} \bar{D}_{k-B+1/k}^j &= G_B D_{k-B+1/k}^j \\ \bar{D}_{k-B+1/k}^j &\sim \left( \mathbf{O}_{B \times 1}, \bar{\Lambda}_B \right) \\ G_B &:= \begin{bmatrix} 1 & \frac{B-1}{B} & \frac{B-2}{B} & \cdots & \frac{1}{B} \\ 0 & 1 & \frac{B-2}{B-1} & \cdots & \frac{1}{B-1} \\ 0 & 0 & 1 & \cdots & \frac{1}{B-2} \\ \vdots & \vdots & \vdots & \ddots & \vdots \\ 0 & 0 & 0 & \cdots & 1 \end{bmatrix} \\ \bar{\Lambda}_B &:= \begin{bmatrix} \frac{B+1}{B} & 0 & \cdots & 0 \\ 0 & \frac{B}{B-1} & \cdots & 0 \\ \vdots & \vdots & \ddots & \vdots \\ 0 & 0 & \cdots & \frac{2}{1} \end{bmatrix} \frac{\Lambda_\rho}{2}. \end{aligned} \quad (15)$$

Combining Eqs. (10), (14) and (15), the block computation formula for the CTS  $T_{k-B+1/k}^j$  is

derived as

$$\begin{aligned} T_{k-B+1/k}^j &= (\bar{D}_{k-B+1/k}^j)^T (\bar{\Lambda}_B)^{-1} (\bar{D}_{k-B+1/k}^j) \\ &= (D_{k-B+1/k}^j)^T (\Lambda_B)^{-1} (D_{k-B+1/k}^j) \end{aligned} \quad (16)$$

where

$$\Lambda_B := [(G_B)^T (\bar{\Lambda}_B)^{-1} (G_B)]^{-1}. \quad (17)$$

As shown in Eqs. (15)-(17), the matrix  $\bar{\Lambda}_B$  for the blockwise computation of  $T_{k-B+1/k}^j$  depends only on the error covariance  $\Lambda_\rho$  and the block size  $B$ . Thus, if  $\Lambda_\rho$  and  $B$  are maintained constant, the matrix  $\bar{\Lambda}_B$  need not be re-calculated once it is computed. A typical implementation structure of the proposed method is depicted in Fig. 1 where the CTSs are utilized to detect the fault-contaminated measurements in computing the receiver's position at each epoch.

### III. MINIMUM DETECTABLE JUMP AND RAMP

The minimum detectable jump (MDJ)  $\mu_{jump}^j$  and the minimum detectable ramp (MDR)  $\mu_{ramp}^j$  are defined as the magnitudes of an abnormal jump and a constant increase in the STDD sequence  $\{d_i^j\}$  that generate the non-centrality parameter  $\lambda_{k-B+1/k}^j$  in the CTS  $T_{k-B+1/k}^j$ . The configurations of MDJ and MDR considered in this study are shown in Fig. 2.

To derive the MDJ and MDR, two important probabilities, probability of false alarm  $P_{FA}$  and probability of missed detection  $P_{MD}$ , should be provided [2,9]. Given  $P_{FA}$ ,  $P_{MD}$ , and the DOF  $B$  of  $\chi^2$ -distributions, the decision threshold  $T_{thresh}^j$  and the non-centrality parameter  $\lambda_{k-B+1/k}^j$  should be computed based on the following definitions [2].

$$\begin{aligned} \int_{T_{thresh}^j}^{\infty} f_{\chi^2(B,0)} &= P_{FA} \\ \int_0^{T_{thresh}^j} f_{\chi^2(B,\lambda_{k-B+1/k}^j)} &= P_{MD} \end{aligned} \quad (18)$$

where  $f_{\chi^2(B,0)}$  and  $f_{\chi^2(B,\lambda_{k-B+1/k}^j)}$  indicates the probability density functions of centralized and non-centralized  $\chi^2$ -distributions.

By Eqs. (3), (12), (13), and (16), the MDJ  $\mu_{jump}^j$  and MDR  $\mu_{ramp}^j$  are derived from the non-centrality parameter  $\lambda_{k-B+1/k}^j$  as follows.

$$\mu_{jump}^j = \left[ \frac{\lambda_{k-B+1/k}^j}{\max_{i \in \{1,2,\dots,B\}} (e_i^T \Lambda_B^{-1} e_i)} \right]^{\frac{1}{2}}$$

$$\mu_{ramp}^j = \left[ \frac{\lambda_{k-B+1/k}^j}{\zeta_B^T \Lambda_B^{-1} \zeta_B} \right]^{\frac{1}{2}} \quad (19)$$

where  $e_i \in \mathbf{R}^{B \times 1}$  denotes the unit vector whose  $i$ -th element is unity and all the other elements are zero.  $\zeta_B \in \mathbf{R}^{B \times 1}$  in Eq. (20) is defined as

$$\zeta_B := [1 \ 1 \ \dots \ 1]^T. \quad (20)$$

Finally, by utilizing the singular values [8] of  $G_B$  and  $\bar{\Lambda}_B$  shown in Eq. (15), the MDJ and MDR are obtained as

$$\mu_{jump}^j = \left[ \frac{B+1}{2B} \Lambda_\rho \lambda_{k-B+1/k}^j \right]^{\frac{1}{2}} \quad (21)$$

$$\mu_{ramp}^j = \left[ \frac{6}{B(B+1)(B+2)} \Lambda_\rho \lambda_{k-B+1/k}^j \right]^{\frac{1}{2}}. \quad (22)$$

Given fixed  $P_{FA}$  and  $P_{MD}$ , it can be verified that the MDJ  $\mu_{jump}^j$  stays near a constant value and the MDR  $\mu_{ramp}^j$  decreases as  $B$  increases due to different growing rate of the denominators as compared with the numerators. This means that the detection resolution against multipath and other soft faults can be improved if we increase  $B$ , i.e., the number of successive measurements.

#### IV. EXPERIMENT

To evaluate the performance of the proposed CTS in real-time standalone positioning, an experiment is performed. To generate an intentional multipath phenomenon, a reflective material is used as shown in Fig. 3. To compare the detection performance of the CTS, the well-known parity method is used as reference fault detection method.

In computing the epoch-by-epoch position solution, only the pseudoranges determined as normal are combined in least square sense. The de-weighting method [6] is not adopted here to concentrate on comparing multipath detection performance. In computing the CTS, the pseudorange variance is set as 0.5 m and the carrier-phase variance is set as 0.005 m. In implementing the parity method, the pseudorange error variance is set as 5 m. Different sets of error variances are used because the CTS can extract receiver noise terms from other error sources while the parity method cannot discriminate among various error sources. During the 600 seconds experiment, total 6 satellites were visible. Thus, the DOF of the  $\chi^2$ -distribution by the parity method

is fixed as 2. In computing the CTS, ten and thirty successive STDDs are used. Thus, the DOFs of the  $\chi^2$ -distribution by the proposed method are fixed as 10 and 30, respectively.

Fig. 4 shows the parity vector magnitude, the CTS using thirty successive measurements of satellite 1 which is apparently affected by multipath, and the CTS using thirty successive measurements of satellite 6 which is unaffected by multipath, respectively. The trend of the other CTSs are not depicted since they are similar to the lowest plot of Fig. 4. As shown in Fig. 4, both the parity vector magnitude and the CTS with respect to satellite 1 fluctuates which implies the existence of multipath. By comparing the upper two plots, it can be seen that the proposed method is more sensitive to multipath. This good characteristic is resulted from the fact that the CTS can only reflect the effects of noise and multipath error among other error sources.

After the multipath is detected by the parity method, identification procedure is followed, i.e., the multipath-affected channel is identified and eliminated in forming a position solution. Since the proposed method is based on channelwise detection, it does not require additional identification procedure. By applying the false alarm rate of 10 %, both methods decided that only the measurements with respect to satellite 1 are affected by multipath throughout the experiment.

Fig. 5 shows the error distributions of the instantaneous least-square position solutions by applying (a) no fault detection method, (b) the parity method, (c) the proposed detection method with 30 successive data. By observing the result of (a), the multipath occurrence can be verified since the position error changes largely along a specific direction. By comparing the results of (b) and (c), it can also be concluded that the proposed method generates less error along the apparent multipath direction as compared with the parity method. Fig. 6 shows the position error magnitudes versus time. As shown in the figure, the position solutions by the proposed detection method show better performance than the position solutions by the parity method due to more successful multipath detection.

## V. CONCLUSION

An efficient channelwise test statistic for single-frequency Global Positioning System receivers was proposed. To evaluate the efficiency of the proposed test statistic, minimum detectable jump and minimum detectable ramp are derived. It was shown that the minimum detectable ramp can be reduced if we increase the number of measurements for computing the



proposed test statistic. An experiment result confirmed that the proposed channelwise test statistic performs well under actual multipath environment.

#### ACKNOWLEDGMENT

This work has been supported by the Automatic Control Research Center (ACRC) and the BK21 SNU-KU Research Division for Information Technology, Seoul National University, and by the Agency for Defense Development (ADD).

## REFERENCES

- [1] M. A. Sturza and A. K. Brown, "Comparison of Fixed and Variable Threshold RAIM Algorithms," in *Third International Technical Meeting of the Institute of Navigation*, pp. 439–443, 1990.
- [2] R. G. Brown and G. Y. Chin, "GPS RAIM: Calculation of Threshold and Protection Radius Using Chi-Square Methods—A Geometric Approach," in *Global Positioning System*, Vol. V, pp. 155–179, The Institute of Navigation, 1997.
- [3] C. J. Comp and P. Axelrad, "Adaptive SNR-based Carrier Phase Multipath Mitigation Technique," in *IEEE Transactions on Aerospace and Electronic Systems*, Vol. 34, No. 1, pp. 264–276, 1998.
- [4] T. Jülg, "Evaluation of Multipath Error and Signal Propagation in a Complex Scenario for GPS Multipath Identification," in *IEEE 4th International Symposium on Spread Spectrum Techniques and Applications*, Vol. 2, pp. 872–876, 1996.
- [5] M. S. Braasch, "Isolation of GPS Multipath and Receiver Tracking Errors," *Journal of the Institute of Navigation*, Vol. 41, pp. 415–434, 1995.
- [6] S. B. Bisnath and R. B. Langley, "Pseudorange Multipath Mitigation by Means of Multipath Monitoring and De-weighting," in *IEEE 4th International Symposium on Kinematic Systems in Geodesy, Geomatics and Navigation*, pp. 392–400, 2001.
- [7] B. W. Parkinson and J. J. Spilker Jr., *Global Positioning System: Theory and Applications Vol. II*. American Institute of Aeronautics and Astronautics, 1995.
- [8] K. Zhou, J. C. Doyle, and K. Glover, *Robust and Optimal Control*. Prentice-Hall, 1996.
- [9] Y. Bar-Shalom and T. E. Formann, *Tracking and data association*. ACADEMIC PRESS, 1988.

## List of Figures

Fig. 1 System structure that utilize channelwise test statistic in epoch-by-epoch positioning

Fig. 2 Configuration of minimum detectable jump and minimum detectable ramp

Fig. 3 Experimental setup

Fig. 4 Comparison of parity vector magnitude, proposed test statistic of multipath-affected channel, and proposed test statistic of multipath-free channel

Fig. 5 Comparison of error distribution in position calculation at each epoch

Fig. 6 Comparison of error distance in position calculation at each epoch

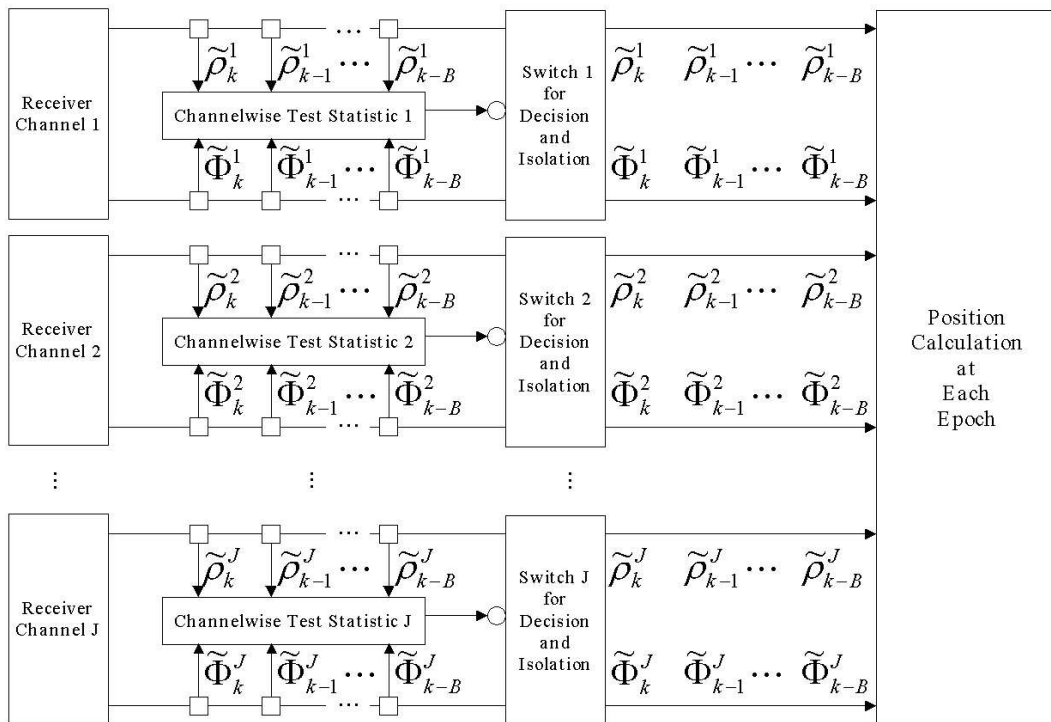


Fig. 1. System structure that utilize channelwise test statistic in epoch-by-epoch positioning

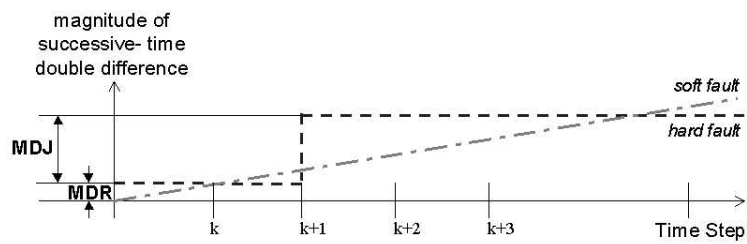


Fig. 2. Configuration of minimum detectable jump and minimum detectable ramp

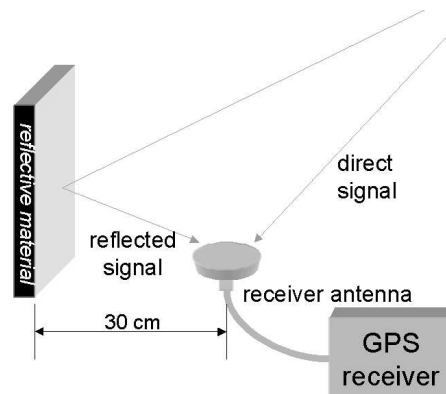


Fig. 3. Experimental setup

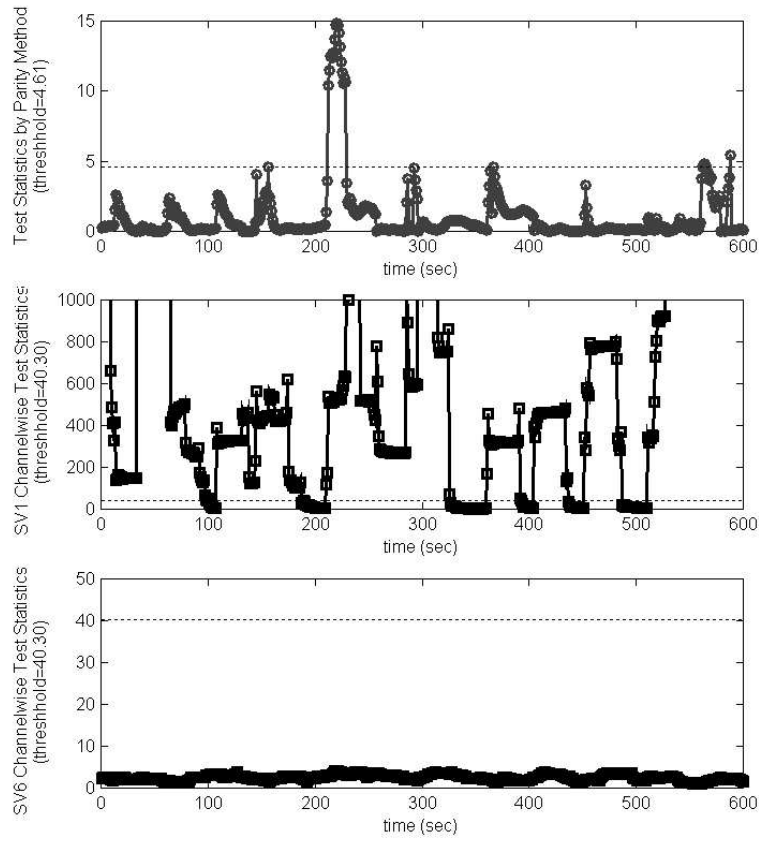


Fig. 4. Comparison of parity vector magnitude, proposed test statistic of multipath-affected channel, and proposed test statistic of multipath-free channel

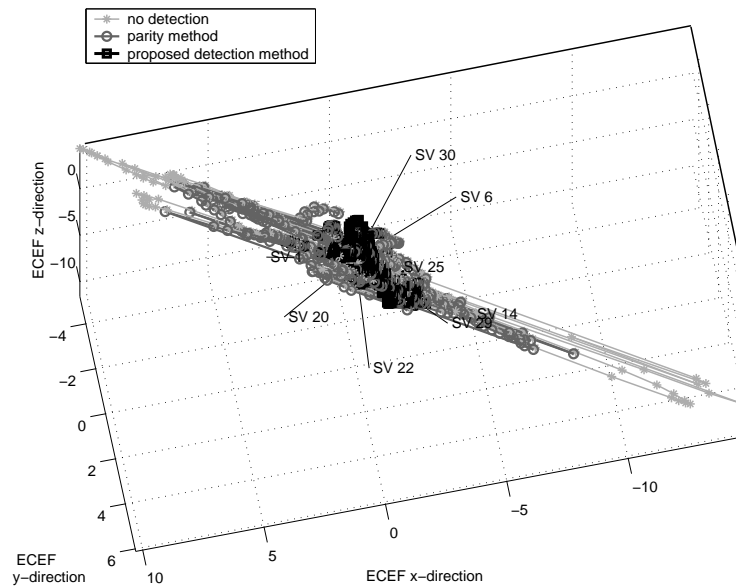


Fig. 5. Comparison of error distribution in position calculation at each epoch

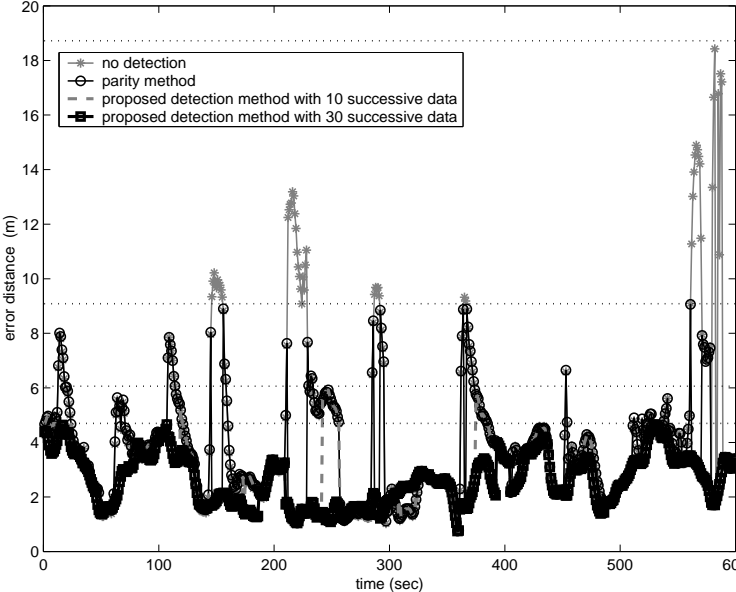


Fig. 6. Comparison of error distance in position calculation at each epoch